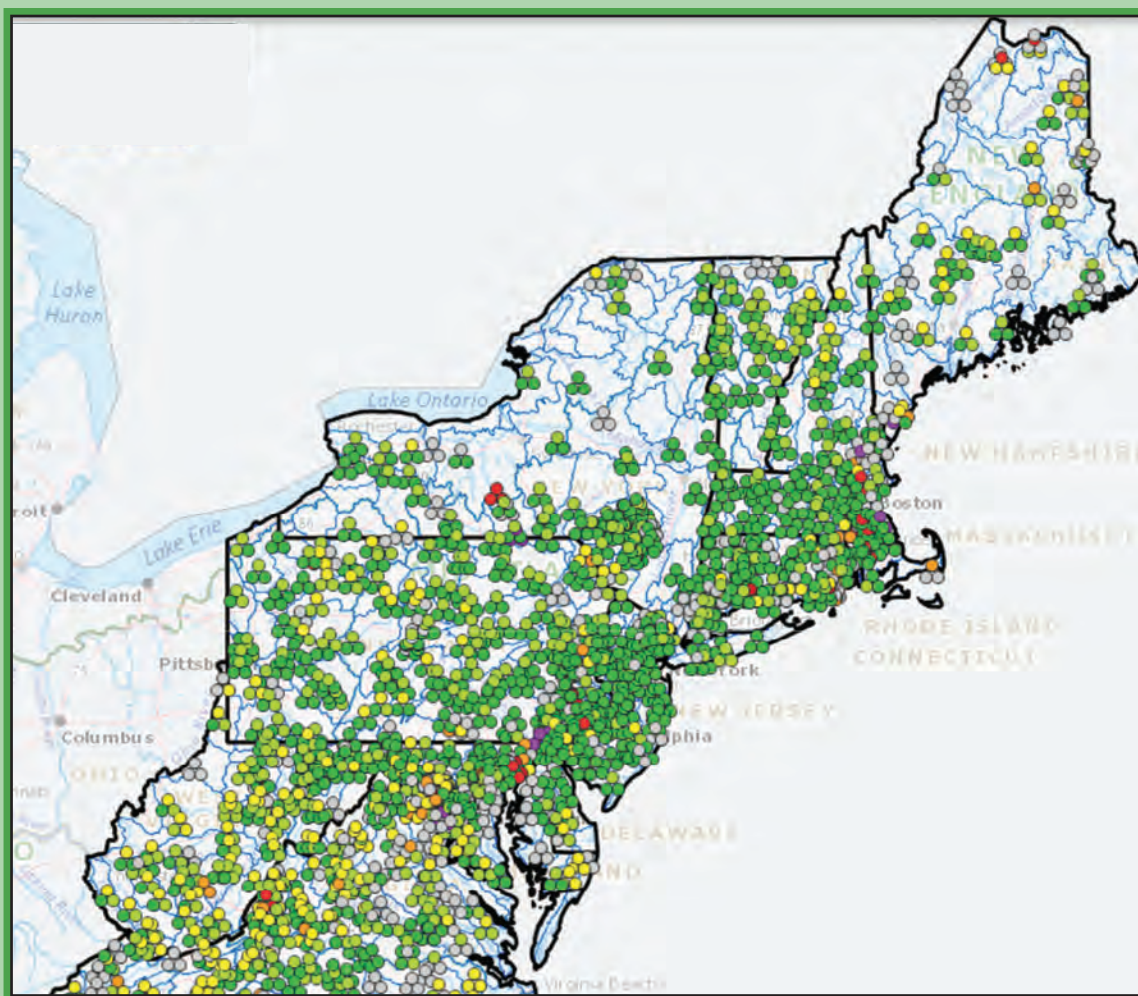


Forecasting Drought Probabilities for Streams in the Northeastern United States



Scientific Investigations Report 2021–5084

Cover. An example of the online interactive map resource tool that provides real-time access to, and visualization of, streamflow drought probabilities.

Forecasting Drought Probabilities for Streams in the Northeastern United States

By Samuel H. Austin

Scientific Investigations Report 2021–5084

U.S. Department of the Interior
U.S. Geological Survey

U.S. Geological Survey, Reston, Virginia: 2021

For more information on the USGS—the Federal source for science about the Earth, its natural and living resources, natural hazards, and the environment—visit <https://www.usgs.gov> or call 1–888–ASK–USGS.

For an overview of USGS information products, including maps, imagery, and publications, visit <https://store.usgs.gov/>.

Any use of trade, firm, or product names is for descriptive purposes only and does not imply endorsement by the U.S. Government.

Although this information product, for the most part, is in the public domain, it also may contain copyrighted materials as noted in the text. Permission to reproduce copyrighted items must be secured from the copyright owner.

Suggested citation:

Austin, S.H., 2021, Forecasting drought probabilities for streams in the northeastern United States: U.S. Geological Survey Scientific Investigations Report 2021–5084, 11 p., <https://doi.org/10.3133/sir20215084>.

Associated data for this publication:

Austin, S.H., 2021, Terms, statistics, and performance measures for maximum likelihood logistic regression models estimating hydrological drought probabilities in the northeastern United States (2019): U.S. Geological Survey data release, <https://doi.org/10.5066/P9E3SK56>.

ISSN 2328-031X (print)

ISSN 2328-0328 (online)

Contents

Abstract.....	1
Introduction.....	1
Methods.....	1
Streamflow Drought Criteria	2
Streamflow Site and Data Selection	2
Streamflow Drought Probability	2
Streamflow Model Development	3
Streamflow Model Verification, Diagnostics, and Cross-Validation	5
Streamflow Drought Probability Results.....	8
Summary.....	8
Conclusions.....	11
Acknowledgments.....	11
References Cited.....	11

Figures

1. An example Maximum Likelihood Logistic Regression model and companion Receiver Operating Characteristic Validation Curve with an area under curve of 0.81, indicating high prediction accuracy, estimating drought streamflow probability in August as a function of mean daily streamflow from the previous February	3
2. An example of the online interactive map resource tool that provides real-time access to, and visualization of, streamflow drought probabilities.....	4
3. Curves illustrating cross-validation receiver operating characteristic results from three-way partitioning of a basin dataset	6
4. Four example receiver operating characteristic curves plotting true positive rate against false positive rate.....	7
5. Best area under the curve values associated with a maximum likelihood logistic regression equation estimating drought streamflow probability in each northeastern United States study basin	10

Tables

1. Rates of correct prediction testing for July, August, and September 2019 by lagged February 2019, maximum likelihood logistic regression streamflow drought probability equations on July, August, and September 2019 data	9
2. Statistics summarizing maximum likelihood logistic regression streamflow drought probability receiver operating characteristic curve best area under the curve values in the northeastern United States.....	9

Conversion Factors

U.S. customary units to International System of Units

Multiply	By	To obtain
Length		
foot (ft)	0.3048	meter (m)
mile (mi)	1.609	kilometer (km)
Area		
acre	0.4047	hectare (ha)
square foot (ft ²)	0.09290	square meter (m ²)
square mile (mi ²)	259.0	hectare (ha)
square mile (mi ²)	2.590	square kilometer (km ²)
Volume		
gallon (gal)	0.003785	cubic meter (m ³)
cubic foot (ft ³)	0.02832	cubic meter (m ³)
acre-foot (acre-ft)	1,233	cubic meter (m ³)
Flow rate		
acre-foot per day (acre-ft/d)	0.01427	cubic meter per second (m ³ /s)
foot per second (ft/s)	0.3048	meter per second (m/s)
cubic foot per second (ft ³ /s)	0.02832	cubic meter per second (m ³ /s)
Hydraulic gradient		
foot per mile (ft/mi)	0.1894	meter per kilometer (m/km)

Temperature in degrees Celsius (°C) may be converted to degrees Fahrenheit (°F) as

$$^{\circ}\text{F} = (1.8 \times ^{\circ}\text{C}) + 32.$$

Temperature in degrees Fahrenheit (°F) may be converted to degrees Celsius (°C) as

$$^{\circ}\text{C} = (^{\circ}\text{F} - 32) / 1.8.$$

Datum

Vertical coordinate information is referenced to the North American Vertical Datum of 1988 (NAVD 88).

Horizontal coordinate information is referenced to North American Datum of 1983 (NAD 83).

Altitude, as used in this report, refers to distance above the vertical datum.

Abbreviations

AUC	area under the curve
FN	false negative
FP	false positive
FPR	false positive rate of prediction
MLLR	Maximum Likelihood Logistic Regression
n	actual negative outcome
N	sum of all negative values
NWIS	USGS National Water Information System
p	actual positive outcome
P	sum of all positive values
PN	predicted negative outcome
PY	predicted positive outcome
P[No]	probability of not exceeding a drought streamflow threshold
P[Yes]	probability of exceeding a drought streamflow threshold
ROC	Receiver Operating Characteristic
TN	true negative
TNR	true negative rate of prediction
TP	true positive
TPR	true positive rate of prediction
USGS	U.S. Geological Survey

Forecasting Drought Probabilities for Streams in the Northeastern United States

By Samuel H. Austin

Abstract

Maximum likelihood logistic regression (MLLR) models for the northeastern United States forecast drought probability estimates for water flowing in rivers and streams using methods previously identified and developed. Streamflow data from winter months are used to estimate chances of hydrological drought during summer months. Daily streamflow data collected from 1,143 streamgages from April 1, 1877, through October 31, 2018, are used to provide hydrological drought streamflow probabilities for July, August, and September as functions of streamflows during October, November, December, January, and February. This allows estimates of outcomes from 5 to 11 months ahead of their occurrence. Models specific to the northeastern United States were investigated and updated. The MLLR models of drought streamflow probabilities utilize the explanatory power of temporally linked water flows. Models with strong drought streamflow probability correct-classification rates were produced for streams throughout the northeastern United States. A test of northeastern United States drought streamflow probability predictions found that overall correct-classification rates for drought streamflow probabilities in the northeastern United States exceeded 97 percent when predicting July 2019 drought probability using February 2019 monthly mean streamflow data. Using hydrological drought probability estimates in a water-management context informs understandings of possible future streamflow drought conditions in the northeastern United States, provides warnings of potential future drought conditions, and aids water-management decision making and responses to changing circumstances.

Introduction

When rainfall is lower than normal over an extended period, streamflows decline and hydrological drought can occur. Droughts often reduce the amount of water available for societal needs and ecological health such as supplies for public and private drinking-water systems, farming, industry, and maintenance of water quantity and quality in natural ecosystems. Recent droughts in the northeastern United States

have highlighted the need for new scientific tools to forecast the probability of future droughts so water managers and the public can be better prepared for these events when they happen. A recent U.S. Geological Survey (USGS) study provides tools that can forecast the probabilities of summer droughts for streams and rivers (Austin and Nelms, 2017). These tools provide promising methods for identifying and anticipating probable streamflow droughts specific to the northeastern United States. Water Science Centers affiliated with the USGS in the northeastern United States have acted together to use these methods for numerous streamflow gages and to make the results of the analyses available on the world wide web. This report describes the drought forecasting technique used to predict droughts for streamflow in the northeastern United States. A companion USGS data release (Austin, 2021) provides the model parameters used in the predictions.

Methods

Participating USGS northeast region Water Science Centers identified a subset of 1,169 USGS gaged basins as being of particular interest to cooperative users, stakeholders, and USGS Science Centers with respect to streamflow drought probabilities. Methods described by Austin and Nelms (2017) were used to prepare updated equations and drought-forecasting management tools for 1,143 of these gaged basins in the northeastern United States. The selected basins were determined as having sufficient data for the development of meaningful predictions. The equations and forecasting tools use statistical modeling approaches to allow anticipation and planning for potential streamflow droughts from 5 to 11 months in advance of their occurrence.

Statistical analyses called Maximum Likelihood Logistic Regression (MLLR) models were prepared for each gaged stream in the study. The probability of an event occurrence is calculated based on the predictors (explanatory variables) used in each model. Each stream-forecast model provides hydrological drought streamflow probabilities for summer months using streamflow data collected during previous months.

Streamflow Drought Criteria

Austin and Nelms (2017) describe hydrological drought as “a deficit in streamflow that may be conceptualized as a period of below normal water flow or depleted reservoir storage—an interval in which streamflow is deficient for a number of consecutive months.” A monthly 20th-percentile streamflow threshold is adopted as a useful indicator of hydrological drought based on criteria that include the necessity to avoid drought streamflows that are exceedingly rare (less than [$<$]10-percent threshold) or common (30-percent threshold) (Patterson and others, 2013; Austin and Nelms, 2017).

Functions performed by MLLR models (fig. 1) include (1) predicting the chance of a streamflow exceeding a particular drought threshold, (2) describing the odds of a particular outcome using a predictive variable, and (3) estimating probability response as a smooth function of a factor. In each model, the probabilities of daily streamflow exceeding (moving above) and not exceeding (staying below) a 20th-percentile drought threshold during summer (July through September) of a given year are estimated as functions of monthly mean streamflow during the previous winter (October through February). In a previous study, Austin and Nelms (2017) demonstrated that well-formed MLLR models can provide accurate predictions of drought streamflow probability and that some of the best-performing models describe probabilities in areas for which drought is of high concern to water-resource managers. For example, in a previous study, one test of 5,950 predictions of September drought streamflow probabilities across the United States documented an overall rate of correct prediction exceeding 90 percent using streamflow data from the previous October (Austin and Nelms, 2017).

Streamflow Site and Data Selection

Streamflow daily data were analyzed from 1,169 gaged basins identified by USGS northeast region Water Science Centers as being of particular interest to cooperative users, stakeholders, and USGS Science Centers (fig. 2). Most of these gaged basins are listed in version 2 of the USGS “Geospatial Attributes of Gages for Evaluating Streamflow” (GAGES-II) dataset (Falcone, 2011). The GAGES-II basins have had at least 20 complete years of discharge records compiled since 1950 or contain streamgages that are currently active in watersheds within the United States. These basins include reference sites—some of the least-disturbed watersheds in the United States—and nonreference sites that exhibit anthropogenic influences. Streamflow daily values collected from water year 1877 through water year 2018 (ending September 30, 2018) were obtained from the USGS National Water Information System (NWIS) for the 1,169 gaged basins (U.S. Geological Survey, 2018). Of the 1,169 gaged basins, 26 were determined to have insufficient data for developing statistically meaningful MLLR equations, in which probabilities are identified within an acceptable range of error. Drought

probability equations were developed for the remaining 1,143 study sites. The period of record for the 1,143 study sites ranged from 10 to 142 years with a mean of 59 years, median of 61 years, and standard deviation of ± 31 years.

Streamflow Drought Probability

An MLLR was used to predict the chance of streamflow exceeding or not exceeding a particular drought streamflow threshold. This chance identifies the odds of a particular drought outcome using one or more predictive variables and estimating probability response as a smooth function of a factor. In this study, the probabilities of streamflow exceeding (moving above) and not exceeding (staying below) a 20th-percentile drought streamflow threshold during summer months are estimated as functions of mean streamflow during previous months. The 20th-percentile threshold is determined empirically from flow values encompassing the full period of record for each site; this threshold is a useful indicator of hydrological drought based on criteria that avoid drought streamflows that are exceedingly rare ($<$ 10-percent threshold) or common (30-percent threshold). An MLLR is applied to the time series from each study site, yielding site-specific equations which describe relations predicting summer month (July, August, and September) drought probability using mean streamflow during each antecedent explanatory month (October, November, December, January, and February). An S-shaped logistic function is used to fit the probabilities. See the more detailed discussion of methods provided by Austin (2014).

Each MLLR binary response has two possible outcomes. For drought streamflow, the binary response indicates whether or not a 20th-percentile drought streamflow threshold will or will not be exceeded. A [Yes] response indicates the drought streamflow threshold will be exceeded—daily streamflow will be greater than the drought streamflow threshold amount. A [No] response indicates a drought streamflow threshold will not be exceeded—daily streamflow will be less than the drought streamflow threshold amount. An MLLR curve is fitted using the difference in the logs of the two probabilities of binary response, expressed as a linear function of a factor variable: mean streamflow during one or more previous months. The linear model may be written as in equation 1, where p denotes the probability of [Yes], $1 - p$ denotes the probability of [No], B_0 , B_1 , and X identify intercept, slope, and explanatory variable respectively. Streamflow drought probabilities are identified for time intervals ranging from 5 to 11 months ahead of potential drought occurrence.

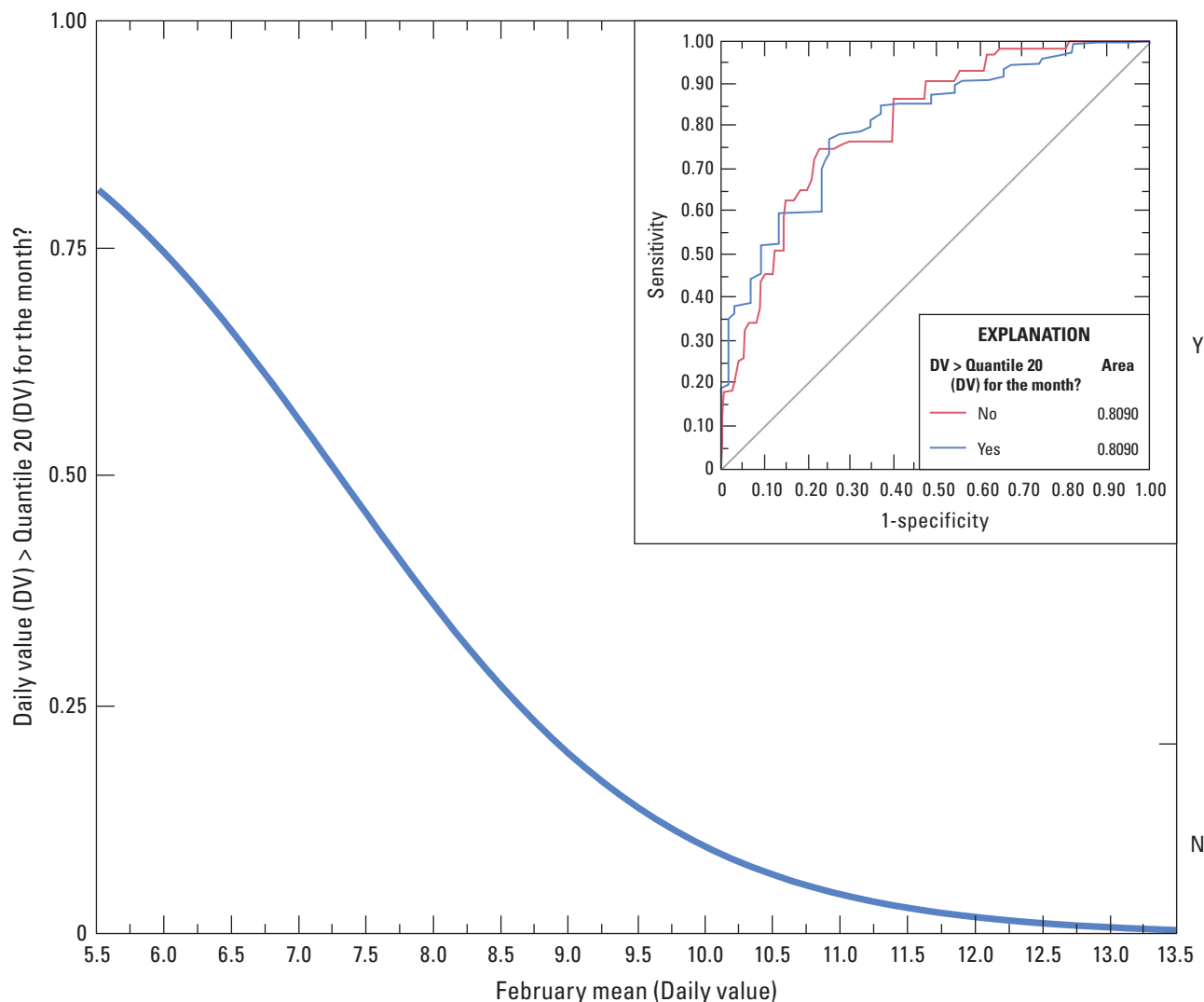


Figure 1. An example Maximum Likelihood Logistic Regression model and companion Receiver Operating Characteristic Validation Curve (inset) with an area under curve of 0.81, indicating high prediction accuracy, estimating drought streamflow probability in August (y-axis) as a function of mean daily streamflow from the previous February (x-axis). Station number 01303000, Mill Neck Creek at Mill Neck, New York, 1937–2018. Daily value [DV] is the average streamflow during a single day, measured in cubic feet per second; Y, the probability of DV exceeding drought flow [no drought], y-axis fraction above the regression line; N, the probability of DV not exceeding drought flow [drought], y-axis fraction below the regression line).

$$\log(p) - (1 - p) = B_0 + B_1 \cdot X \quad \text{or} \quad \log\left(\frac{p}{1-p}\right) = B_0 + B_1 \cdot X \quad (1)$$

Streamflow Model Development

For streamflow models, the probabilities of two response levels are fitted using a logistic function: nominal Y responses to a linear model of X terms. Variable coefficients (Bs) are chosen to maximize the joint probability attributed by the model to the responses that occur. This iteratively minimizes the negative log-likelihood of each outcome—P[Yes] and

P[No]—over the range of explanatory variable (X) values, as the negative log-likelihood values converge to final estimates (SAS Institute Inc., 2012). Minimizing negative log-likelihood is equivalent to maximizing log-likelihood, yielding MLLR probabilities (Hosmer and Lemeshow, 2000). The explanatory (X) term in each streamflow model represents the mean monthly streamflow(s) associated with the preceding month(s). Each model describes the chance of a particular streamflow

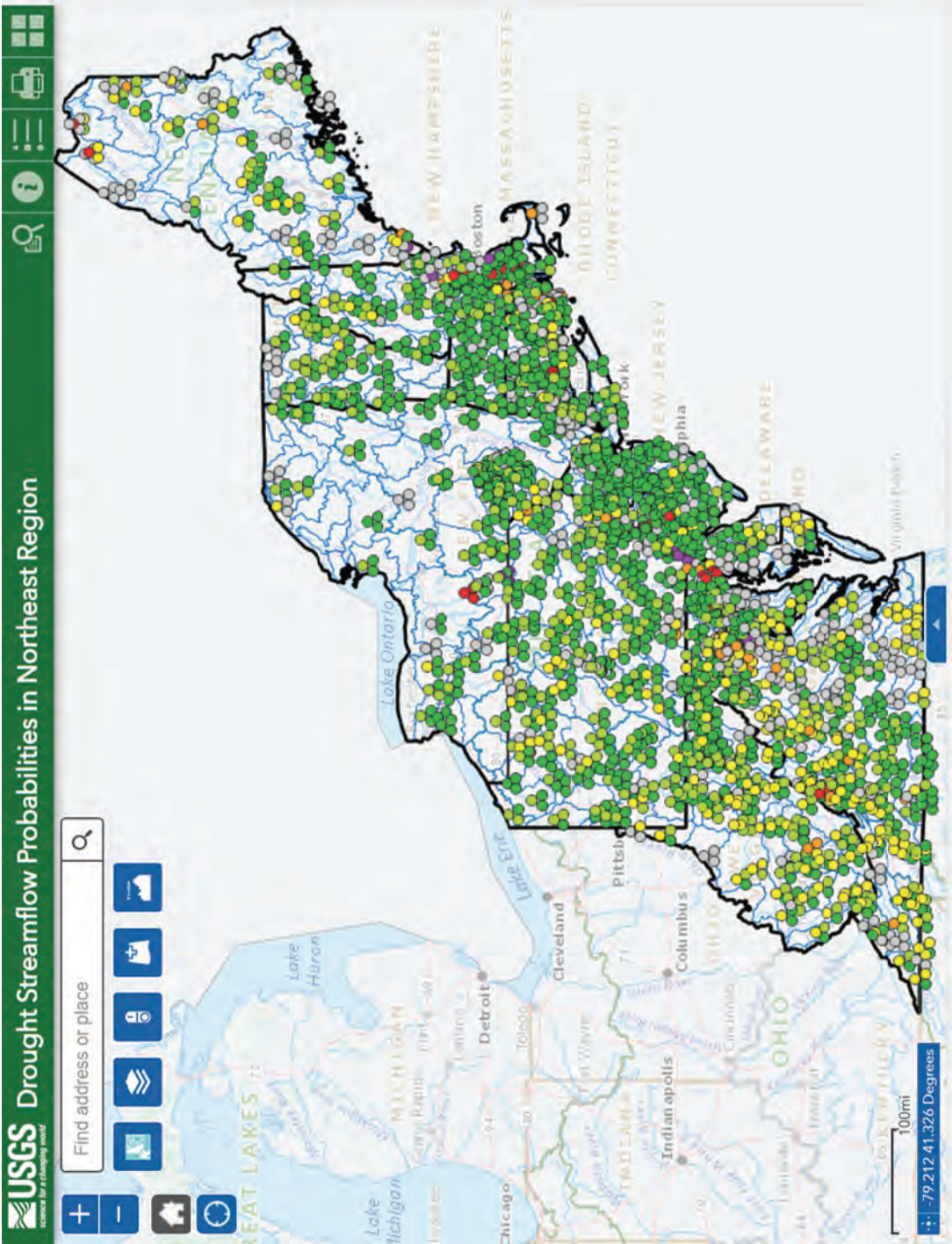


Figure 2. An example of the online interactive map resource tool that provides real-time access to, and visualization of, streamflow drought probabilities. Gaging stations are shown. Drought probability values for each gaging station are illustrated as a triad of three color-coded circles representing drought estimates for July (top circle), August (right most circle), and September (left most circle). Custom symbology is used to display three summer month streamflow drought probabilities for each streamgage. Drought months are selected interactively by the user. Drought probability values are shown using a color-coded scale of seven probability classes and an eighth no-data class. Green dots indicate lower drought probabilities. Yellow and orange dots indicate higher drought probabilities. Red and purple dots indicate highest drought probabilities. Gray dots indicate no available data. Only results from statistically significant relations are presented (p-value ≤ 0.05). Equations with p-values greater than 0.05 are identified as having no-data and are colored gray. (Kandel and others, 2019).

exceeding or not exceeding a drought threshold expressed as a percentile of all streamflow measured at a streamgage over the period of record.

Streamflow Model Verification, Diagnostics, and Cross-Validation

Visual inspections of streamflow MLLR model response curves, evaluations of MLLR p-values, and Receiver Operating Characteristic (ROC) curves are used to verify, diagnose, and validate models. Predicted y-values define a probability distribution of the response, correct for either of the two outcomes (Sall and others, 2007).

A probability value (p-value) for each streamflow MLLR model describes the strength of the probability distribution relative to the likelihood that the evaluated occurrence could simply be a product of chance. Each p-value is determined using a likelihood ratio chi-square test of the hypothesis that all regression parameters are zero (Sall and others, 2007). P-values are computed taking twice the difference in negative log-likelihoods between the results of the fitted streamflow MLLR model and the results of a reduced version of the streamflow model with no explanatory variable. Each p-value identifies the probability of obtaining a greater chi-square value by chance alone, as if the streamflow model fit was no better than that of a reduced model containing only intercepts. A low p-value ($p < 0.05$) indicates a statistically significant model. Multicollinearity and autocorrelation can be associated with time series. In MLLR models, multicollinearity is a property of multiple explanatory (x) variables, not dependent (y) variables, and is therefore of concern only if MLLR models have more than one x variable, which is not the case for the streamflow models in this study.

Autocorrelation (the correlation between the elements of a time series and other elements of the same time series that have been separated by a certain time interval) may also be associated with streamflow time series. In this study, two chi-square tests help identify (1) streamflow-model significance and (2) any influences associated with autocorrelation. A likelihood ratio chi-square test comparing the log-likelihood of the fitted model with the log-likelihood of a model with no explanatory (x) variable (an intercept-only model) is used to identify the statistical significance of the whole streamflow MLLR model. A second chi-square test identifies the significance of the estimates made using the explanatory (x) variable. The chi-square p-values reported by this test indicate explanatory (x) variable significance. A significant whole-model chi-square test, together with a significant explanatory (x) variable chi-square test, indicates a significant streamflow model with an insignificant influence of autocorrelation upon the explanatory (x) variable (Allison, 2012).

Persistence is also often associated with autocorrelation in a streamflow time series. The degree of persistence may be identified by the rate at which an autocorrelation function decays over time. It is likely that persistence—along

with other affects associated with the timing of water moving through a basin by way of soil, subsoil, vegetation, groundwater, streamflow, snowmelt, and myriad pathways of varying size and length—contributes to aggregate delays and dynamics approximating a first-order system response and helps determine the probabilities identified in our streamflow MLLR models (Forrester, 1971).

Streamflow models were developed using three-way partitioning, and cross-validation was used to evaluate each MLLR model. Each basin's dataset was divided into three randomly selected subgroups (partitions), each representing one-third of the basin's complete dataset. For each basin, streamflow models were developed using the first partition, streamflow model parameters were estimated on the second partition, and streamflow model predictive abilities were tested on the third partition. To display and compare test results and evaluate streamflow model accuracy and predictive power, ROC curves were used (fig. 3).

Actual positive outcomes (p) and actual negative outcomes (n) may be compared to predicted positive outcomes (PY) and predicted negative outcomes (PN). Comparisons of actual outcomes and predicted outcomes identify instances of true positive (TP), false positive (FP), false negative (FN), and true negative (TN) predictions convenient for cross-validation and evaluation of predictive power. If an instance is actually positive (p) and is predicted as positive (PY), it is identified as a TP outcome. If an instance is actually positive (p) and is predicted as negative (PN), it is identified as a FN outcome. If an instance is actually negative (n) and is predicted as negative (PN), it is identified as a TN outcome. If an instance is actually negative (n) and is predicted as positive (PY), it is identified as a FP outcome. The sum of all positive values (P), therefore, is $TP + FN$ and the sum of all negative values (N) is $FP + TN$.

For each streamflow MLLR model, it is useful to understand and compare the rates at which true positive, true negative, false positive, and false negative predictions are made. Sensitivity is a term used to identify the true positive rate of prediction (TPR), which may be calculated as TP/P . The term specificity is used to identify the true negative rate of prediction (TNR), which may be calculated as TN/N . It follows that $1 - \text{specificity}$ is the false positive rate of prediction (FPR), which may be calculated as FP/N . Sensitivity (TPR) answers the question, "If the streamflow model predicts a positive event, what is the probability that it actually is positive?" Specificity (TNR) answers the question, "If the streamflow model predicts a negative event, what is the probability that it really is negative?" $1 - \text{specificity}$ (FPR) answers the question, "If the streamflow model predicts a positive event, what is the probability that it is making a mistake?"

An FPR–TPR x-y plot generates an ROC curve with the vertical axis showing the proportion of TP results that are correctly identified and the horizontal axis showing the proportion of FP results that are misidentified as TP results. Thus, graphs of ROC curves depict relative tradeoffs between benefits (TPs) and costs (FPs). One point in ROC space is considered better than another if it is positioned above and to the left of the first

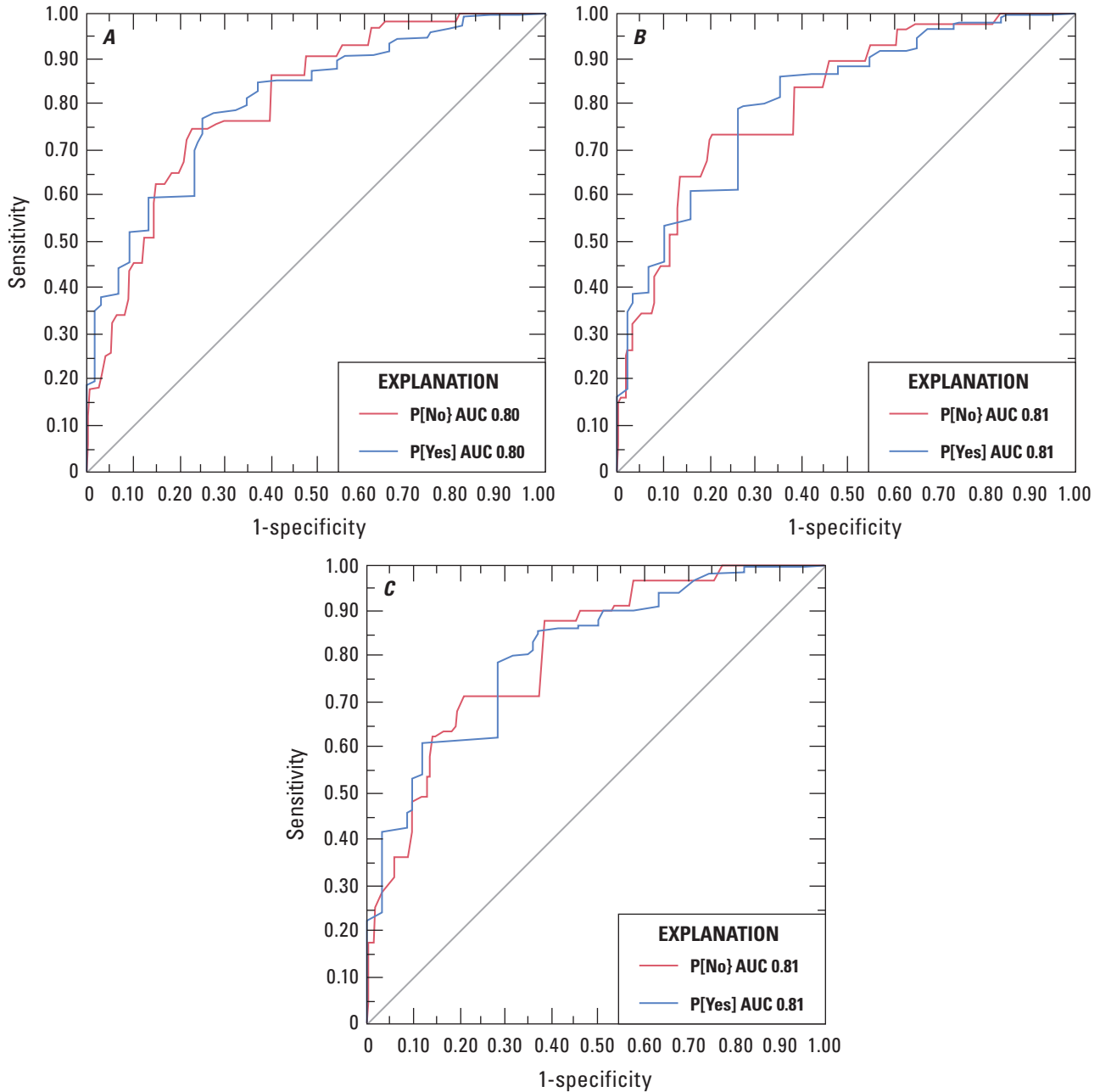


Figure 3. Curves illustrating cross-validation receiver operating characteristic (ROC) results from three-way partitioning of a basin dataset. Sensitivity (the true positive rate) is plotted against 1-specificity (the false positive rate). Graph *A* shows ROC results for the model development partition. Graph *B* shows ROC results for the parameter estimation partition. Graph *C* shows ROC results for the predictive test partition. Station number 01303000, Mill Neck Creek at Mill Neck, New York, 1937–2018. (P[No], probability of not exceeding a drought streamflow threshold; P[Yes], probability of exceeding a drought streamflow threshold; AUC, area under the curve. The gray line bisecting each plot identifies the position at which P[No] and P[Yes] would be equivalent to one another.)

with higher TPR and lower FPR. The ROC curves are insensitive to changes in class distribution, so if the proportion of positive to negative instances changes in a test set, the ROC curves will not change. This important property enables visualizing and organizing classifier performance without regard to class distributions or error costs, which is useful with skewed distributions (Fawcett, 2006).

An ROC curve is a two-dimensional depiction of classifier performance and, to compare classifiers, it is often useful to reduce ROC performance to a single scalar value representing expected performance. This is commonly done by calculating the “area under the curve” (AUC) of each ROC curve as an index of streamflow model strength (Allison, 2012). As it is a portion of the area of a unit square, with both axes of a ROC curve ranging from 0 to 1, AUC has a value between 0 and 1. In this ROC space, a perfect classifier—passing through the point (0,1) and indicating 100 percent TPR results and 0 percent FPR results—has an AUC of 1 (line D, [fig. 4](#)). A random classifier, in which TPR results and FPR results are split

evenly (50 percent each), has an AUC of 0.5 (line A, [fig. 4](#)). [Figure 4](#) lines B and C illustrate incremental improvements in classification rates when compared to [figure 4](#) line A. ROC curves with higher AUC values are preferred.

An AUC also has a probabilistic interpretation, depicted as $AUC = P[\text{random positive example} > \text{random negative example}]$. The AUC equals the probability that a random positive example is greater than a random negative example. In other words, the AUC is the probability that the classifier will assign a higher score to a randomly chosen positive case than to a randomly chosen negative case. This facilitates focus on the strength of the positive case probabilities, which are associated with the question we are asking. An AUC value was prepared for each streamflow MLLR equation and used to compare and rank model equations based on model strength. A streamflow model with a comparatively high AUC, among the streamflow models prepared for each site, has been selected to represent each site.

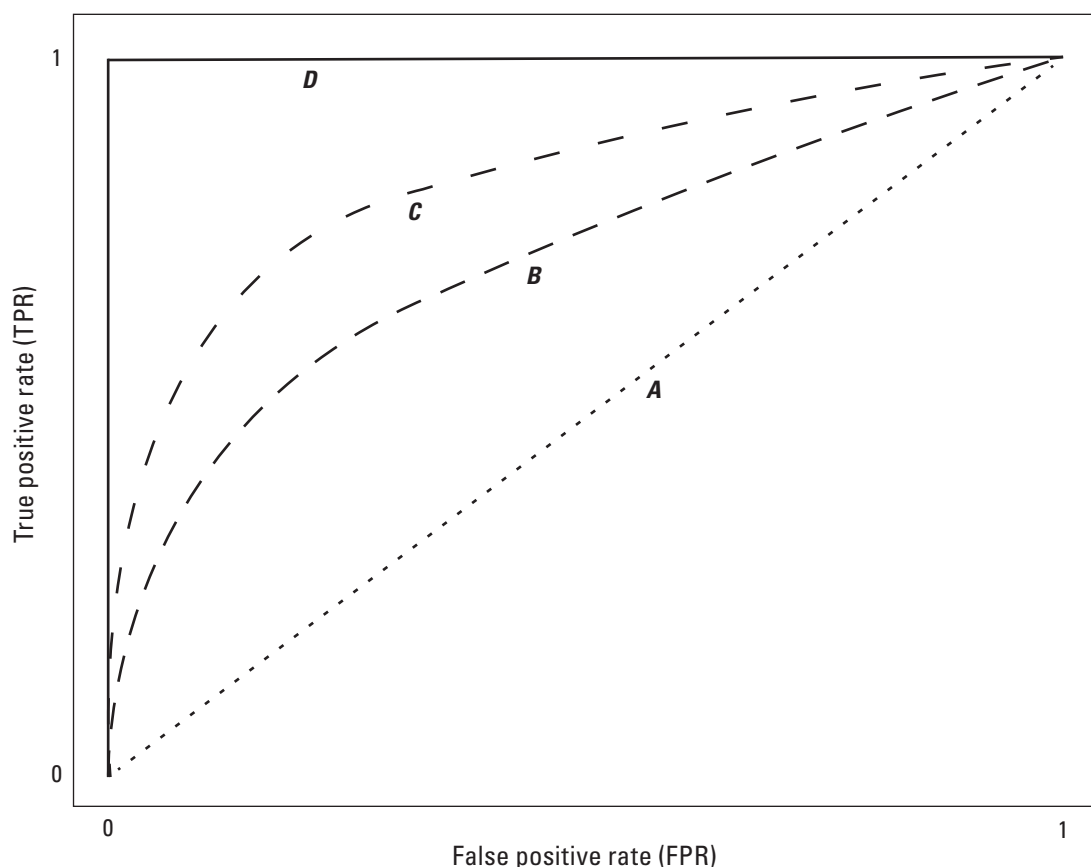


Figure 4. Four example receiver operating characteristic (ROC) curves plotting true positive rate (TPR) against false positive rate (FPR). Curve A is equivalent to a random classifier in which TPR and FPR are split evenly (50 percent and 50 percent). Curves B and C illustrate incremental improvements in classification rates. Curve D is equivalent to a perfect classifier in which TPR equals 100 percent and FPR equals 0 percent.

Streamflow Drought Probability Results

As a real-world test of streamflow model utility and equation prediction strength—in addition to testing cross validation, ROC development, and AUC analysis—estimates of July 2019 hydrological drought streamflow probability were made as a function of February 2019 mean daily streamflow using MLLR equations for 952 gaged study basins. These basins represent a subset of the total 1,143 basins, containing all basins for which July 2019 and February 2019 streamflow values had been recorded in NWIS at the time the test was performed. These drought events were chosen for this comparison because summer 2019 drought events were the most recent for which drought probabilities were calculated. Predicted probabilities using equations based on NWIS data (which are provisional and subject to revision) were compared to the actual July 2019 daily streamflow values in each basin. Probabilities were identified as correct if the probability of exceeding drought streamflow was greater than (less than) 0.5 and paired with an actual July 2019 daily streamflow value greater than (less than) the July 20th-percentile drought streamflow threshold for the basin.

Of the 952 predictions made using July 2019 by February 2019 equations, 921 (97 percent) were correct and 31 (3 percent) were incorrect when compared to actual streamflow values (table 1). This same comparison was also made for August 2019 and September 2019 hydrological drought streamflow probabilities and tested against actual August 2019 and September 2019 streamflow values. Both August 2019 and September 2019 comparisons were estimated using MLLR equations employing February 2019 mean daily streamflows. The August 2019 correct prediction rate exceeded 95 percent, with 901 correct predictions and 51 (5 percent) incorrect predictions. The September 2019 correct prediction rate exceeded 85 percent, with 810 correct predictions and 142 (15 percent) incorrect predictions (table 1).

Figure 1 shows the plot of an example equation estimating drought streamflow probability in August as a function of mean daily streamflow from the previous February. To demonstrate determining drought streamflow probabilities for a particular (x) value, figure 1 is entered vertically from the x-axis to the blue regression line, then exited horizontally to the y-axis where probability values are read. For example, an x-axis February mean (daily value) of 6 cubic feet per second (ft^3/s) yields a y-axis probability of not exceeding drought streamflow in August of 75 percent, and an inferred probability of exceeding drought streamflow in August ($1-0.75$) of 25 percent.

In this study, 92 percent of all equations prepared exhibit correct classification rates superior to a random classifier (AUC values ≥ 0.6). The equations with AUC values of 0.7 or higher have a 96 percent correct classification rate (table 2). The strongest predictive equations are associated with basins in Delaware, New York, and Pennsylvania (median best AUC values of 0.73, 0.73, and 0.73, respectively) and the weakest equations are associated with basins in West Virginia (median best AUC value of 0.68). The best AUC values in each study basin are shown as dots in figure 5. The highest AUC values—represented by darker red dots in figure 5—are found in large portions of the northeastern United States, particularly center portions of the mid-Atlantic and northeastern states spanning Virginia, Maryland, Pennsylvania, New York, Connecticut, and Massachusetts. Table 2 lists statistics summarizing AUC values. Additional detailed results and supporting data are available in an accompanying USGS data release (Austin, 2021).

Summary

This study provides streamflow probabilities specific to the northeastern United States, building on previous work (Austin, 2014; Austin and Nelms, 2017) and demonstrating the utility of using well-formed linear regression models to estimate streamflow drought probabilities. As in previous studies, preparation of well-formed MLLR models estimating summer month hydrological drought streamflow probabilities from streamflow data collected during previous months provides information useful to managers and decision makers and allows them the opportunity to anticipate and plan for potential future streamflow conditions. Modeling hydrological drought streamflow probabilities in this way exploits the explanatory power of temporally linked water flows, even without full knowledge of the nature and timing of surface and groundwater flows specific to each basin and stream.

Much of this explanatory power may be a product of overall water flow through each basin, approximating a first-order system response (Forrester, 1971). As water flow through a basin is delayed by physical processes associated with each flowpath in the basin (such as friction, varying surface- and groundwater flowpath lengths and sinks, soil matrix potential), water resides in the basin for a time and the discharge rates associated with accumulated water are the temporally linked information that each model exploits. When predicting streamflow probabilities, the effects of this fundamental first-order response may outweigh the influences from other shorter-term or recurring impacts such as changes in dam operations, agricultural effects, and land use decision rules (Austin and Nelms, 2017).

Table 1. Rates of correct prediction testing for July, August, and September 2019 by lagged February 2019, maximum likelihood logistic regression streamflow drought probability equations on July, August, and September 2019 data.

[\leq , less than or equal to; $>$, greater than]

Response (y)	Explanatory variable (x)	Gages in test	Total correct predictions	Total incorrect predictions	Rate of correct prediction (percent)	Rate of incorrect prediction (percent)
July 2019 drought probability ≤ 0.5 or > 0.5	February 2019 monthly mean streamflow	952	921	31	97	3
August 2019 drought probability ≤ 0.5 or > 0.5	February 2019 monthly mean streamflow	952	901	51	95	5
September 2019 drought probability ≤ 0.5 or > 0.5	February 2019 monthly mean streamflow	952	810	142	85	15

Table 2. Statistics summarizing maximum likelihood logistic regression streamflow drought probability receiver operating characteristic curve best area under the curve (AUC) values (≥ 0.6) in the northeastern United States.

State	Gages in sample	Model equations in sample	Mean of best AUC values	Median of best AUC values	Minimum of best AUC values	Maximum of best AUC values	Standard deviation of best AUC values
Connecticut	50	594	0.71	0.70	0.60	0.94	0.08
Washington, D.C.	2	19	0.71	0.70	0.61	0.86	0.08
Delaware	14	233	0.75	0.73	0.60	0.97	0.10
Massachusetts	63	640	0.72	0.70	0.60	0.98	0.09
Maryland	123	1,738	0.73	0.72	0.60	0.99	0.09
Maine	44	418	0.71	0.69	0.60	0.98	0.09
New Hampshire	29	325	0.74	0.72	0.60	0.99	0.10
New Jersey	77	989	0.73	0.72	0.60	0.94	0.09
New York	111	1,253	0.74	0.73	0.60	0.99	0.10
Pennsylvania	210	2,435	0.74	0.73	0.60	0.99	0.10
Rhode Island	21	231	0.71	0.70	0.60	0.94	0.08
Virginia	270	4,068	0.73	0.72	0.60	0.99	0.09
Vermont	31	325	0.70	0.69	0.60	0.92	0.08
West Virginia	98	1,032	0.71	0.68	0.60	0.95	0.08

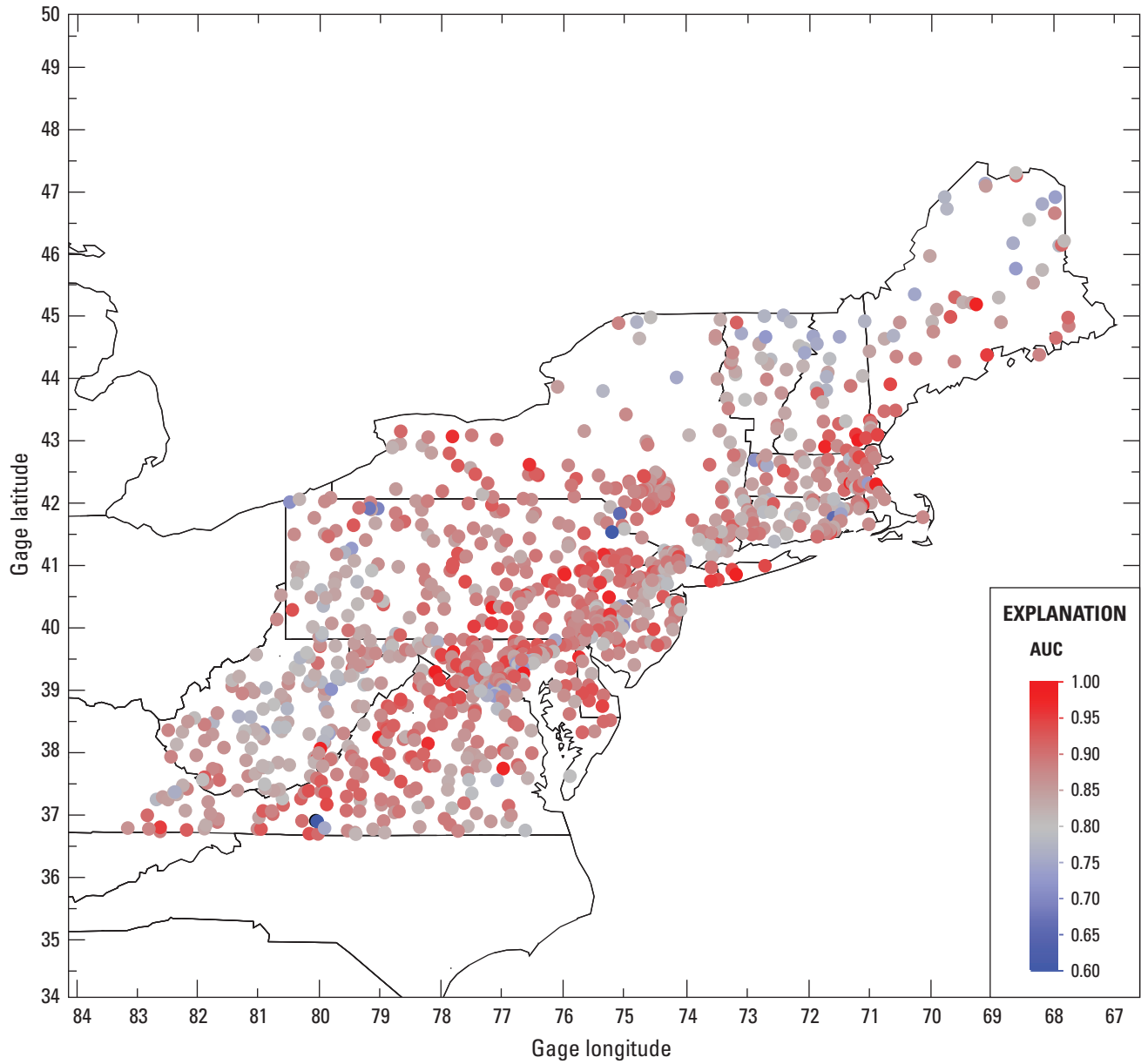


Figure 5. Best area under the curve (AUC) values associated with a maximum likelihood logistic regression equation estimating drought streamflow probability in each northeastern United States study basin. Values range from 0.60 (indicating 60-percent correct-classification rates of drought streamflow probabilities) to 1.00 (indicating 100-percent correct-classification rates of drought streamflow probabilities).

Conclusions

Concerns about risks of hydrological drought are likely to grow as global climate warms and new weather patterns potentially disrupt expected streamflow rates. As these changes occur, advanced warnings of probable streamflows become increasingly important. Few past studies have specifically forecast hydrological droughts. Equations prepared for this publication provide basin-specific empirical estimates of hydrological drought probabilities unique to the northeastern United States using data collected at USGS streamgages over a period of record spanning April 1, 1877, through October 31, 2018, with a median gage-record length of 61 years.

Equations may be used to inform water-management decision making, which helps to mitigate the effects of hydrological drought. Predictions of probable hydrological drought outcomes up to 11 months in advance of occurrence provide opportunities for managers to communicate local and regional hydrological drought conditions, improve drought awareness, implement drought-management plans at appropriate times, and test water-allocation protocols and decision rules before potential crises develop. Continued work to improve predictive-model performance using new and optimized combinations of hydrological drought threshold percentiles and explanatory variables will help further leverage the explanatory power of these models, which helps drive progress and continuous improvement in assessing and predicting hydrological drought in the northeastern United States.

Acknowledgments

Mark Bennett, George E. Harlow, Jr., and Keith Robinson of the U.S. Geological Survey are thanked for their support and enthusiasm for this project and for their helpful advice and review of this report.

References Cited

- Allison, P.D., 2012, Logistic regression using SAS—Theory and application (2d ed): Cary, N.C., SAS Institute Inc., 339 p.
- Austin, S.H., 2014, Methods for estimating drought streamflow probabilities for Virginia streams: U.S. Geological Survey Scientific Investigations Report 2014–5145, 20 p., March 2019 at <https://doi.org/10.3133/sir20145145>.
- Austin, S.H., 2021, Terms, statistics, and performance measures for maximum likelihood logistic regression models estimating hydrological drought probabilities in the northeastern United States (2019): U.S. Geological Survey data release, <https://doi.org/10.5066/P9E3SK56>.
- Austin, S.H., and Nelms, D.L., 2017, Modeling summer month hydrological drought probabilities in the United States using antecedent flow conditions: *Journal of the American Water Resources Association*, v. 53, no. 5, p. 1133–1146, accessed November 15, 2018, at <https://doi.org/10.1111/1752-1688.12562>.
- Falcone, J.A., 2011, GAGES-II: Geospatial attributes of gages for evaluating streamflow: U.S. Geological Survey Unnumbered Series, accessed December 2013 at <https://doi.org/10.3133/70046617>.
- Fawcett, T., 2006, An introduction to ROC analysis: *Pattern Recognition Letters*, v. 27, no. 8, p. 861–874. [Also available at <https://doi.org/10.1016/j.patrec.2005.10.010>.]
- Forrester, J.W., 1971, Principles of systems: Cambridge, Mass., Productivity Press.
- Hosmer, D.W., and Lemeshow, S., 2000, Applied logistic regression (2d ed.): Hoboken, N.J., John Wiley and Sons, Inc., 383 p. [Also available at <https://doi.org/10.1002/0471722146>.]
- Kandel, C., Austin, S.H., and Rapp, J.L., 2019, Drought streamflow probabilities in Northeast Region: U.S. Geological Survey WebMapping Application, accessed April 3, 2019, at https://va.water.usgs.gov/webmap/drought_ne/.
- Patterson, L.A., Lutz, B.D., and Doyle, M.W., 2013, Characterization of drought in the South Atlantic, United States: *Journal of the American Water Resources Association*, v. 49, no. 6, p. 1385–1397. [Also available at <https://doi.org/10.1111/jawr.12090>.]
- Sall, J., Greighton, L., and Lehman, A., 2007, JMP start statistics—A guide to statistics and data analysis using JMP (4th ed): Cary, N.C., SAS Institute Inc., 628 p.
- SAS Institute Inc., 2012, JMP 10 modeling and multivariate methods: Cary, N.C., SAS Institute Inc., 702 p.
- U.S. Geological Survey, 2018, USGS water data for the Nation: U.S. Geological Survey National Water Information System database, accessed December 3, 2018, at <https://waterdata.usgs.gov/nwis>.

For additional information, contact:

Director, Virginia and West Virginia Water Science Center
U.S. Geological Survey
1730 East Parham Road,
Richmond, Virginia 23228

Or visit our website at <https://www.usgs.gov/centers/va-wv-water>

Publishing support provided by the U.S. Geological Survey Science
Publishing Network, West Trenton Publishing Service Center.

